Feasibility of Assessing Trabecular Bone Architecture by Intermolecular Double-Quantum Coherence MRI

C-L. Chin[1], X. Tang[2], L-S. Bouchard[3], P. K. Saha[1], W. S. Warren[3], F. W. Wehrli[1]

[1]University of Pennsylvania Medical Center, Philadelphia, PA, United States, [2]University of Nevada, Reno, NV, United States, [3]Princeton University, Princeton, NJ, United States

Introduction

The signal generated by distant dipolar interactions can be explained as resulting from the distant dipolar field that leads to the generation of multiple spin echoes [1]. The phenomenon has also been interpreted in terms of intermolecular multiple-quantum coherence (*i*MQC) [2]. Since this signal arises mainly from remotely coupled spins separated by the correlation distance, D_c, [2], *i*MQC offers the potential to probe structures by varying D_c [2-4]. Here, we investigate the feasibility of applying *i*MQC MRI for probing trabecular bone structure at a spatial resolution that simultaneously permits the direct quantification of trabecular network architecture. Thus, the information obtained from *i*MQC images can be validated with structural parameters derived from the high-resolution images. We first demonstrate with a modified double-quantum CRAZED (α-τ/2-{γG_cT}-π-τ/2-β-{2γG_cT}-TE/4-π-TE/2-π-TE/4-*Acq.*) imaging sequence and 4-step phase cycling (PC) [4] that the *i*MQC signals generated from various coherence pathways yield predictable signals in *k*-space. Subsequently, we apply this approach to assess trabecular bone architecture.

Materials and Methods

K-Space Signal Analysis for Various Coherence Pathways

For spins evolving with coherence order M during the τ period, the residual *k*-value, Δk_C^M, arising from the pair of correlation gradients [4], can be expressed as

$$\Delta k_C^M = (2-M)\times\frac{\gamma G_c T}{2\pi} = \frac{(2-M)}{2D_c} \qquad (1)$$

where G_c and T are the amplitude and duration of the correlation gradient, γ is the gyromagnetic ratio, and $D_c=\pi/(\gamma G_c T)$. The maximum values of k_x and k_y in 2D *k*-space are given as, $k_{x,y}^{MAX}=N_{x,y}/2FOV_{x,y}$, where $FOV_{x,y}$ and $N_{x,y}$ are the field-of-view and the number of encoding steps along either *x* or *y* direction. When $\Delta k_C^M \le k_{x,y}^{MAX}$, the phase of the spurious signals will be unwound by the spatial encoding gradients; thus leading to refocusing at a location shifted with respect to the center of *k*-space by $\Delta n_{x,y}^M$ pixels,

$$\Delta n_{x,y}^M = \frac{\Delta k_c^M}{k_{x,y}^{MAX}}\times\frac{N_{x,y}}{2} = (2-M)\times\frac{FOV_{x,y}}{2D_c} \qquad (2)$$

iDQC Bone Imaging

Cylindrical trabecular bone specimens from the human distal radius were cored (2.5 cm diameter/1.2 cm thick) and the marrow removed. The samples, wrapped with Parafilm® and placed in saline-filled cylindrical plastic vials (principal axis of trabecular elements ⊥ B_o), were imaged at 4T (GE Signa™) using a modified double-quantum CRAZED pulse sequence with 4-step PC and β=π/6 [4]. In this manner, signal generated via various coherence transfer pathways, M=0 (ZQC), 1(SQC), 2 (DQC), and 3 (TQC), can be isolated. Imaging parameters: TR=5s, TE/τ=200/30ms, FOV=4×4cm, matrix size=256×128, D_c =0.2, 0.5, 0.8, and 1.6mm [the correlation gradient || phase-encoding gradient (*y*-axis)], and slice thickness=2.0mm.

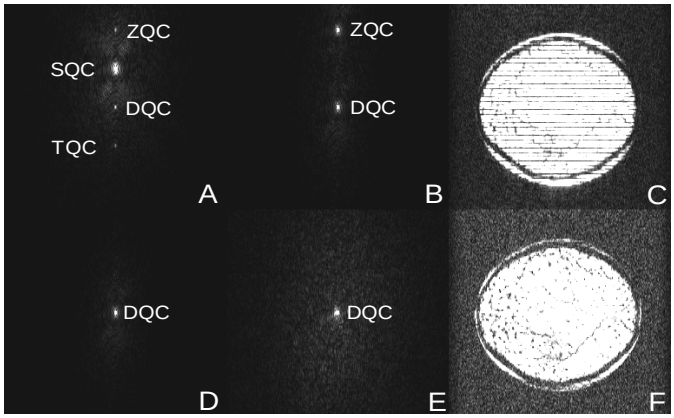

FIG 1 *i*MQC *k*-space data and images of a trabecular bone sample for different PC schemes (D_c=0.8mm): no PC (A), 2-step PC (B) and the corresponding image (C); 4-step PC (D), and no PC (E, the correlation gradient || slice-selection gradient; no spurious echo is observed) and the corresponding image of E (F).

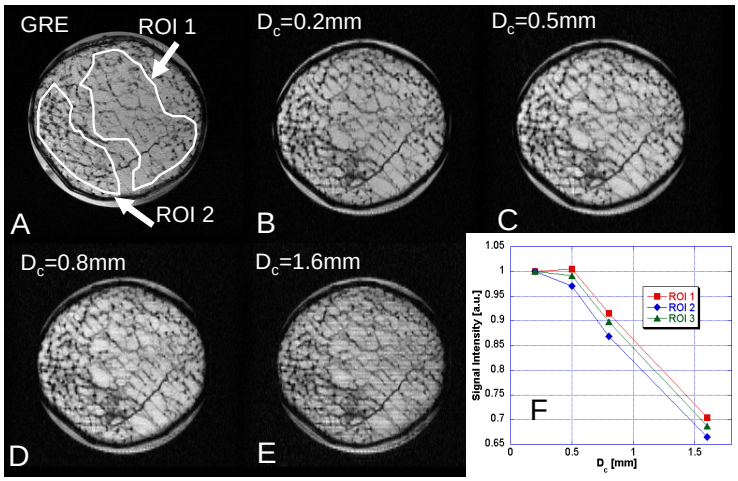

FIG 2 Gradient-echo reference image (pixel size =156×156 μm^2) of the trabecular bone specimen (A). *i*DQC images of trabecular bone acquired at various D_cs (B-E). Signal intensity versus D_c for ROIs indicated in (A) as well as for the average from the entire section (labeled ROI 3) (F).

Results and Discussion

Figure 1 shows the *k*-space data of *i*DQC images obtained with different PC schemes. Based on Eq. [2], the artifactual signal maxima appears at pixel offsets Δn_y =50 (M=0), 25 (M=1), and -25 (M=3) (Fig. 1A). With 2-step PC, significant modulations caused by the ZQC signal contamination exist (Fig. 1C), which can be removed with 4-step PC. Figures 2A-E show the *i*DQC bone images as a function of D_c, and in Fig. 2F the signal is plotted versus D_c for the ROIs indicated in Fig. 2A. It is noted that for the modified CRAZED sequence, image intensity is determined by the density of paired spins separated by D_c, it is thus expected to increase as D_c approaches the mean trabecular spacing. The curve corresponding to ROI 1 suggests a maximum around D_c=0.5mm, not seen for corresponding data from ROI 2 (Fig 2F). Using the fuzzy distance transform method [5], the calculated mean/standard deviation of trabecular spacing distributions are 675/422 μm for ROI 1, and 467/226 μm for ROI 2. The results suggest the feasibility of regional trabecular separation measurements although the relatively coarse sampling of D_c currently limits the achievable accuracy.

Conclusions

This work shows that in double-quantum coherence imaging involving dipolar coupling between distant spins, leakage signals from undesired coherence pathways (ZQC, SQC and TQC). The method may have potential for probing trabecular bone architecture without the need to resolve individual trabecular elements.

References **1**. Bowtell R *et al*, J Magn Res **88**, 643 (1990). **2.** Warren WS *et al*, Science **262**, 2005 (1993). **3.** Capuani F *et al*, Magn Reson Med **46**, 683 (2001). **4**. Chin CL *et al*, Proc. ISMRM 11th Meeting, 803 (2003) **5**. Saha PK *et al*, Computer, Vision, and Imaging Understanding, **86**, 171 (2002).